SYNOPSIS

ON

DESIGN,DEVELOPMENT AND EXPERIMENTAL STUDIES ON MICRO HYDRO PELTON TURBINE.

submitted to Gujarat Technological University

for the Award of

Doctor of Philosophy

in

Mechanical Engineering

By

Chaudhari Anupkumar Hasmukhlal

Enrollment No. 189999919008

Under the supervision of

Dr. Gaurangkumar C. Chaudhari

Assistant Professor,

Mechanical Engineering Department

C.K. Pithawala College of Engineering and Technology (009), Surat.

GUJARAT TECHNOLOGICAL UNIVERSITY, AHMEDABAD

April [2026]

TABLE OF CONTENT

LIST OF FIGURES

LIST OF TABLES

1. TITLE OF THESIS AND ABSTRACT

1.1 TITLE

Design,Development and Experimental studies on Micro hydro pelton turbine.

1.2 ABSTRACT

Micro-hydro power represents one form of renewable energy generation that can be considered to be one of the most dependable and environmentally responsible methods of producing renewable energy as they are ideally suited for sites with a high hydraulic head and low discharge rates having hydraulic head heights of up to 1800m. The turbine technologies available for these conditions, Pelton impulse turbines have historically exhibited greater operational efficiency and better structural integrity than other types of water turbines. The component that comprises the heart of a Pelton turbine is the runner bucket and the maximization of hydraulic performance (i.e., hydraulic efficiency) can be attributed to the careful optimization of specific critical design characteristics such as the speed ratio, exit angle of the bucket, and overall bucket geometry; furthermore, overall hydraulic performance depends directly and solely upon the suppliers of Pelton turbine technology and on the Pelton turbine designer being able to provide these components, which will produce maximum hydraulic performance within the operation of the Pelton turbine. The research Work described here with attempt to fully analyze this problem by utilizing an integrated multi-physics methodology to analyze hydraulic parametric design, perform structural static and modal analysis with finite element modeling using ANSYS Mechanical APDL, conduct steady-state and transient computational fluid dynamics analysis using ANSYS Fluent, fabricate an optimized runner through sand-casting, and perform controlled experimental testing.

A thorough parameteric analysis across both speed ratio and bucket exit angle range has been conducted, validating a peak theoretical hydraulic efficiency of 94.29 percent at the optimum configuration. An F.E.A on four materials, under six combined loading conditions, has determined structural safety in all cases; hence, stainless steel 314 was the material of choice for the bucket based on its superior yield strength, corrosion resistance, and wear properties. A CFD simulation demonstrated clear trends for pressure distribution, flow, and turbluent kinetic energy in the bucket, with agreement to published experimental results. The enhanced runner constructed from sand-casting patterns offered a maximum hydraulic efficiency of

90.92 percent and maximum thrust power of 2018.97 W, greater than that of the conventional modeled runner by 2.05 percentage points in efficiency and 4.37 percent greater thrust power.

2. A brief description on the state of the art of the Research Topic

2.1 Energy Scenario

In 2022, the total percentage of electricity generated globally by energy sources was split. The global share of electricity production was allocated to renewable sources at a collective rate of 27.3 percent, with hydropower accounting for the largest portion of all electricity generation at 15.9 percent—more than either wind or solar power, or any other renewable energy source [2].According to projections released by the International Energy Agency (IEA), hydropower is expected to take over as the leading source of on-demand clean energy (i.e., energy that can be generated on demand) by 2050, with a contribution of more than 40 percent to electricity production (based on a scenario of net-zero emissions) [1].The growing presence of hydropower can be attributed to both its established capacity (i.e., installed generation (or capacity)) and to its unique ability to provide a stable, controllable supply of electricity that can be used in conjunction with variable sources of solar and wind energy generation.

Table 1 Installed Power Generation Capacity in India as of FY 2024-25 [3]

Source	Installed Capacity (GW)	Share (%)
Thermal (Coal, Gas, Oil)	~239	~53
Renewable (Solar, Wind, Small Hydro, Bio)	~159	~35
Large Hydropower	~52	~12
Nuclear	~7.5	~1.7
Total	**~450**	**100**

Table 1 outlines India's total installed generating capacity (in MW) and distribution of generating capacity by type of plant for FY 2024 - 2025 (FY04- FY25). The total installed generated capacity is around 450,000 MW. The India among the top 5 countries (countries with largest hydroelectric generating capacity globally [3].According to estimates, India has about 148,000 MW (148 million MW) of hydropower potential; however, the vast majority of that potential has not been commercially developed and remains available. There is an opportunity to develop small/micro hydro facilities in hills/remote areas, thereby increasing the availability of electricity to those not connected to a national grid.

2.2 Projection: Hydro Power in India

India is experiencing a resurgence in interest and investment into its hydropower sector via newly developed policies that encourage new constructions to take place within the sector. As announced in April 2023, the government of India published its Guidelines for Pumped Storage Hydropower Projects, which establishes a consistent set of rules under which hydropower projects will be built throughout the nation [5]. Based on projections from the Central Electricity Authority, India's currently installed hydropower generation capacity is expected to reach 61.6 gigawatts (GW) by the fiscal year ending March 2029 (2029-30).

In the small hydroelectric portion of the hydropower sector, which consists of plants with an installed capacity of up to 25 megawatts (MW) and is administered by the Ministry for New and Renewable Energy (MNRE), the Alternate Hydro Energy Centre (located at the Indian Institute of Technology (IIT) Roorkee) has prepared an estimate of the total hydroelectric capacity that can be generated from hydropower plants across 7,133 potential development sites on a national scale. This total potential development is estimated to be 21,133 MW, of which only 25 percent have been developed. To help facilitate this development, a total of Rs 2,584.60 crore has been committed towards the implementation of the Small Hydro Power Development Scheme (2026-31), which is intended to support approximately Rs. 15,000 crore of overall investment into small hydroelectric plant projects in the country. To support the addition of ever larger amounts of variable renewable energy into India's electricity grid [29].

2.3 Pelton Turbine[30]

The Pelton wheel is an impulsive-type hydraulic turbine created by American engineer Lester Allan Pelton in the 1870s that transforms kinetic energy from the sudden release of water via high-velocity jets into mechanical work through a rotating shaft. Pelton's turbine differs from reaction turbines such as Francis and Kaplan turbines, which operate under the pressure of hydraulics for the entire time their fans are turning. The Pelton turbine has no hydraulic work on its fan blades; all pressure energy supplied by the water is converted into kinetic energy prior to the water jet hitting the fan blades. The high-velocity jet of water hits the fan blades in a tangential direction — using only kinetic energy to turn the shaft.

Pelton's innovative design of the double-dish bucket allows for a near-kinetic state (no residual velocity) of the escaping water when the fan tips are rotating at approximately 50% of the speed of the incoming water jet, resulting in maximum transfer of available kinetic energy to the shaft. Pelton's design created one of the most volume-efficient hydraulic machines ever; thus, making the Pelton turbine the ideal choice at sites with low-discharge and high-head, which are typically found in mountainous areas.

3. Brief Literature Status on Pelton Turbine

As hydropower continues to grow as a major source of energy worldwide, the design and performance optimisation of Pelton turbines has attracted significant research activity. There is a remarkable consensus among the published literature that there are no universal designs for Pelton turbines and therefore researchers have taken many approaches to develop and identify various designs, including optimisation of hydraulic design, assessment of structural integrity, erosive and wear behaviour and the use of computational fluid dynamics in modelling[17].

From a design standpoint, the performance of Pelton turbines can be affected by many design parameters (i.e., speed ratio, specific speed, bucket exit angle, number of buckets) [9, 10]. Results from various studies indicate that the optimal speed ratio for maximum efficiency is between 0.46 to 0.50 for most practical applications; similarly, bucket exit angles between 10^0 and 17^0 are generally associated with the best performance [11]. According to several researchers, structural analysis of Pelton Turbines has identified two major locations of stress concentration as a result of jet impact loading: the splitter tip and the concave surface of the bucket [12, 13]. Material selection appears to be a key factor in structural safety margins, as austenitic and martensitic stainless steels have proven to be significantly more reliable than cast iron and aluminium alloys in high-performance, water side applications. Both the Eulerian and the Lagrangian methods are used as computational fluid dynamics approaches to simulate the unsteady multi-phase free-surface flow phenomena within Pelton Power turbine buckets using ANSYS Fluent and ANSYS CFX software[17].Transient three-dimensional analysis provides the most accurate description of the dynamics of the jet flow and the bucket through symmetrical bifurcation occurring at the splitter plate, the pressure build-up occurring at the stagnation point and the smooth deflection of the fluid flow along the bucket's outer profile. However, there is no single study in the current literature that includes a comprehensive parametric geometry optimization study, a multi-material structural finite element analysis study inclusive of modal analysis, a steady-state and transient computational fluid dynamics analysis and formally uncertainty validated testing of the experimental results all within one complete research framework for micro-hydropower applications. For this reason, this study has been conducted to fill this void [31].

4. Definition of Problem

The literature review indicates that the design of Pelton turbine buckets used in micro hydro systems involves a large number of interrelated hydraulic, structural, and material design considerations. Most existing studies published on Pelton bucket designs tend to examine only one or two aspects of these designs in isolation, concentrating solely on design; structural analysis; communications; or CFD modelling without integrating all three into one well-structured research framework. This results in a deficiency in the knowledge base where practitioners lack confidence when designing and testing new Pelton runners for micro hydro applications.

Most existing micro hydro Pelton buckets have geometries that have been derived from the large design of commercial Pelton buckets through a process of empirical scale-up, and do not include parametric optimisation of the buckets geometry so that it will perform optimally with the specific micro hydro site's hydraulic, velocity and other operating conditions. Consequently, many of the Pelton turbines currently in service perform below their theoretical maximum hydraulic efficiency.

In addition to this, there has been little to no work done on examining the performance of Pelton bucket materials under combinations of the static and dynamic loads associated with a Pelton runner, including impact; uniform; non-uniform; and combinations of all three loadings with regard to modes of resonance and the potential for fatigue.

There is therefore a clear multi-dimensional engineering project that is underway. The first challenge consists of completing a methodical parametric study to determine the speed ratio and the bucket exit angle that yield the greatest theoretical hydraulic efficiency for the site of the design. Second, a rigorous finite element analysis of the structural integrity of the design and material shall be conducted to demonstrate that it is safe for all expected operational loads and exhibits no risk of resonance. Third, hydraulic performance will be validated computationally with CFD simulations prior to fabrication.

Fourth, physical performance testing of the enhanced runner ultimately created will be conducted compared to a Conventional runner design and the results will be verified by completing formal uncertainty analysis to confirm that any differences observed are statistically significant and not a result of measurement scatter.

5. Objectives and Scope of Research Work

1. To review existing literature on micro hydro power and Pelton turbine technology, identifying research gaps in integrated design, analysis, and performance validation at the micro hydro scale.
2. To carry out systematic hydraulic design and parametric optimisation of the Pelton turbine bucket geometry.
3. To perform static structural analysis and pre-stress modal analysis of the Pelton turbine bucket in ANSYS Mechanical APDL.
4. To conduct steady-state and transient computational fluid dynamics analysis of the Pelton turbine bucket in ANSYS Fluent,
5. To fabricate the optimized Pelton runner and dynamically balance the complete assembly to ensure accurate and reliable experimental testing.
6. To carry out a comparative assessment between conventional and enhanced Pelton turbines under identical operating conditions to evaluate their performance levels.

This research includes numerical investigations and experimental investigations and has produced an integrated multi-physics design framework linking analytical parametric optimisation, computational structural analyses and flow analyses, physical fabrication and experimentally validated testing for micro hydro Pelton turbine runners.

6. Methodology for Research

The research methods for this study have 6 stages. Each stage builds on previous stages, which helps to provide a clear path that connects hydraulic designs of turbines to experimental validation of each of those designs.

Stage 1 - Hydraulic Design and Parametric Optimization:

Turbine runners were hydraulically performed in a reference microhydro site. Using a Parametric Study over Speed Ratios from 0.445 to 0.485 and Bucket Exit Angles from 10 to 15 Degrees, the Runner Design Configuration yielding Peak Theoretical Power Efficiency was determined.

Stage 2 - Material Selection:

The materials (A390 Aluminum, CA6NM Steel, Structural Steel, and Stainless Steel3214) were evaluated with respect to corrosion resistance, wear performance and mechanical properties. One of these materials was selected as the suitable material for enhanced design of bucket exit angle.

Stage 3 - Finite Element Analysis (FEA) of Structures Using ANSYS Mechanical APDL: Interesting base analysis and pre-stressed modal analysis of each structural bucket (in horizontal and vertical position) using multiple loads applied simultaneously, and the verification of the analysis was performed before final simulations of the design elements were conducted.

Stage 4 - Computational Fluid Dynamics (CFD) Analysis Using ANSYS Fluent:

Using the Standard (k–ε)Turbulence Model, the flow pattern within the internal body of the bucket will be determined using steady-state CFD analysis and inlet velocities, and transient CFD simulations of a rotating full bucket runner at the design operating conditions will be determined using a sliding mesh interface.

Stage 5 - Fabrication:

Through the use of 3D-printed patterns, the runner has been manufactured through metal sanding. Each bucket has been inspected and machined at the face of the bucket to the runner, and combined, the runner has been dynamically balanced.

Stage 6 - Experimental Testing:

Performance testing has been conducted on conventional and enhanced pelton runner at five nozzle openings on a custom built closed-loop hydraulic test rig.uncertainty analysis has been conducted (ASME PT62-012014) along with a statistical evaluation to validate the Results.

7. Original Contribution by Thesis

The findings of this research contribute significant knowledge to the field of Pelton turbine micro hydro engineering as outlined in the following paragraphs:

1. A systematic parametric investigation was conducted on the parameters of the Pelton turbine buckets to determine which operating point will provide the maximum theoretical hydraulic efficiency based on the combination between the ratio of velocity and the angle of bucket exit. The bucket configuration that produces maximum theoretical hydraulic

efficiency has a speed ratio of 0.485 and an exit angle of 10^0 yielding a peak hydraulic efficiency of 94.29% when combined. Additionally, within this res0earch a new bucket design has been developed that has 38.2% more width, 57.8% longer interior cavity, and 25% greater angle for the splitter than current designs.

2. FEA requirements for static structure and pre-stress modes were completed using ANSYS Mechanical APDL on four materials having six combined loads. The analyses indicate that of the Stainless Steel 314 provides the safest design with respect to the bucket frequency of resonance being 13.4.

3. The performance of the Pelton bucket was evaluated by using steady state and transient CFD analyses in ANSYS Fluent with the results providing details of velocity, pressure and turbulent kinetic energies around the enclosed fluid within the Pelton bucket. Transient analysis was performed with over 21.6 million elements and with a moving mesh, and the results confirmed the splitting of jets in a bilaterally symmetrical manner and that the jets remain smoothly connected to the inside wall throughout their path to the outlet.

4. A Pelton runner that has been improved was manufactured out of Stainless Steel 314 using sand casting to create the 3D patterns which have a 100% tolerance to the complex bi-ellipsoidal bucket cavity, as well as it was dynamically balaced before the test takes place.

5. The statisitical significance of the improvements made to the performance of the enhanced Pelton runner was tested by performing a formal experimental uncertainty analysis in accordance with ASME PTC 22-2014 and ISO GUM. This methodology has not been previously employed in the micro hydro Pelton literature.

8. Achievements with respect to Objectives

8.1 Design Optimisation of Pelton Turbine Bucket

Two parameters are primarily responsible for determining the theoretical hydraulic efficiency of a Pelton turbine, which are: (1) the speed ratio φ, which is defined as the percentage of the bucket tip peripheral velocity to that of the incoming water jet; and (2) the bucket exit angle β at the splitter section. In order to produce smooth water flow over the inner bucket surface and eliminate almost all energy losses through the exit lip, research shows that the bucket exit angle should be between 10 to 20 degrees, and the inlet angle of the splitter should be below 20 degrees.

Table 2 Parametric Efficiency Matrix — Speed ratio vs Hydraulic efficiency

Exit Angle / φ	**0.455**	**0.465**	**0.470**	**0.475**	**0.480**	**0.485**
10°	0.9361	0.9391	0.9404	0.9414	0.9422	0.9429
12°	0.9330	0.9360	0.9373	0.9383	0.9391	0.9398
13°	0.9313	0.9343	0.9355	0.9365	0.9374	0.9381
15°	0.9274	0.9304	0.9316	0.9326	0.9335	0.9341

This study determined the theoretical hydraulic efficiencies of a hydraulic turbine by taking into account speed ratios (0.445 to 0.485) and exit angles (10-15°). Utilizing the analytical equation for determining theoretical hydraulic efficiency [given as $\eta = (u/C_1) \times (1 + k \cdot \cos\beta_2) \times 2 \cdot (1 - u/C_1)$; where k = 0.96, as the relative velocity ratio] recorded the results presented in Table 2 of the report. Results show that, as exit angles decrease, efficiency will increase for all tested speed ratios; the theoretical maximum efficiency obtained is 94.29% at φ = 0.485 with β = 10°.

The relationship between exit angle and efficiency is shown in Figure 1 and appears to be a linear function that provides predictable results; with every 1° reduction in exit angle corresponding approximately to an increase of roughly 0.2 percentage points in hydraulic efficiency. This parametric study designed a new style of bucket having an exit angle of 10° that structurally improved upon the original, including a bucket 38.2% wider than the original design; deeper concave cavities; and larger splitter angles (25% larger than original); all of these will promote better jet capture and improve momentum transfer to runner.

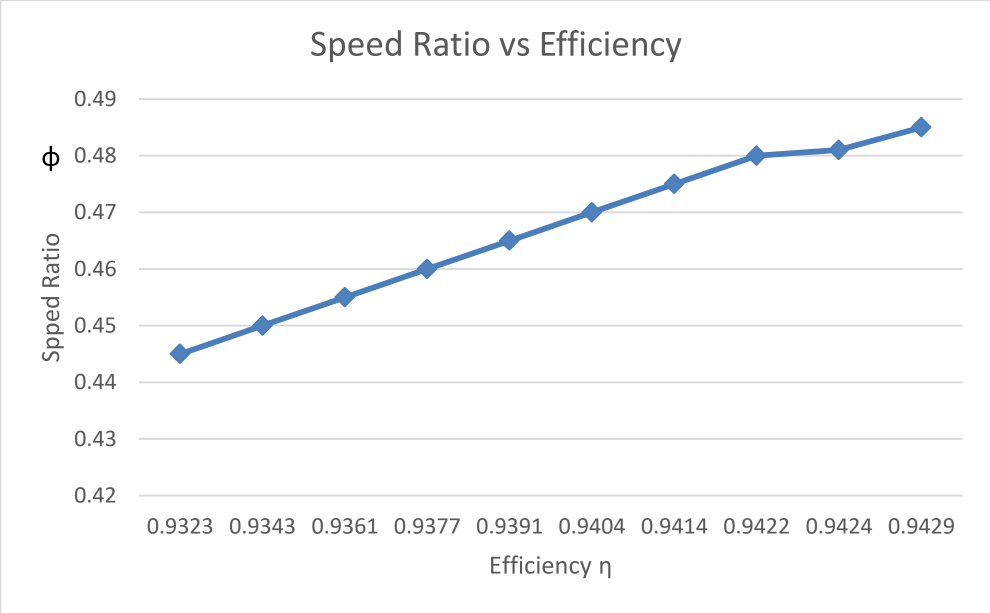

Figure 1 Speed ratio vs Hydraulic efficiency

8.2 Structural and Modal FEA of Pelton Turbine Bucket

ANSYS Mechanical APDL performed analysis on structural finite element analysis of budgets with up to 687,557 nodes and 921,522 elements, where each mesh was grid-independent before running production runs. Two orientations of the Pelton bucket (horizontal (180°) and vertically (90°) were analyzed under six combinations of loads: low impact force (F_1=349N), high impact force (F_2=153.864kN), uniform hydraulic pressure ($P=2.41\times10^5$Pa), two pressure levels that were unequally distributed and the total load includes both forces plus pressures at both levels. The materials used as for the test are shown in Table 3.

Table 3 Material Properties of the Four Proposed Bucket Materials [24]

Property	**CA6NM**	**Str. Steel**	**A390 Al**	**SS 314**
Density (kg/m³)	7,800	7,850	2,700	7,750
Young's Modulus (GPa)	200	200	75	193
Yield Strength (MPa)	689	250	180	586
Ultimate Strength (MPa)	827	460	180	207

Figure 2 The stripe contours at the lower impact point (F_1=349N) show the horizontal bucket and the four candidates all have relatively small deformations due to buckling of most of these types of materials; however, A390 aluminum has the maximum deformation because its elastic modulus is only 75 GPa compared to the rest of the four materials. Also , under the larger measurement of (F_2=153.864kN), as seen in the stripe contours, there is some striking evidence that will correspond to the maximum deformation at the tips. i.e., a total of 16.5mm at the end of the horizontal bucket. In both cases the deformation patterns will produce results consistent with the expected result based on the manner of how the jet applies force on the buckets and confirm that the structural model has accurately captured the forces acting on the buckets.

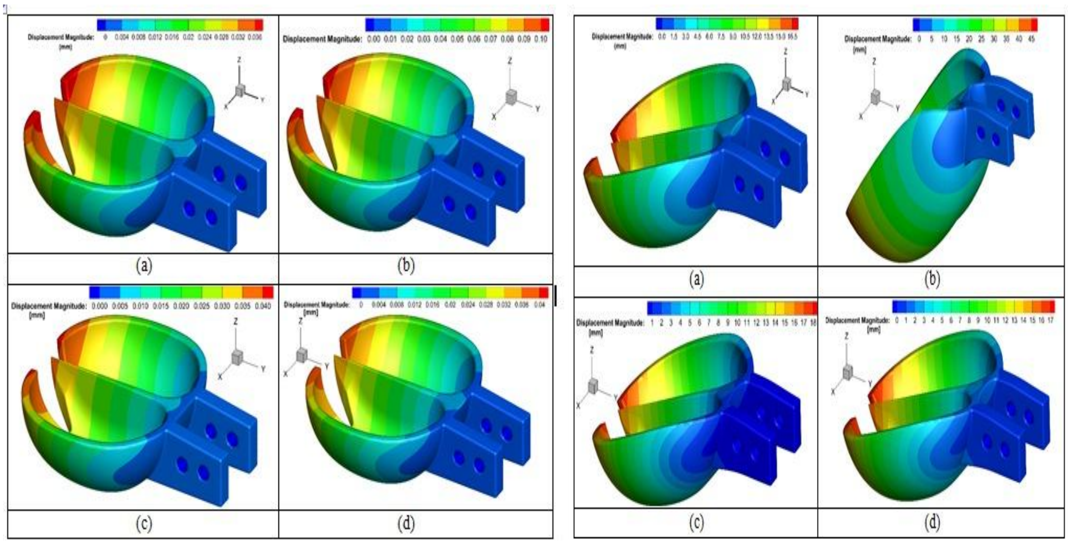

Figure 2 Structural deformation contours of horizontal bucket for F_1 = 349 N (left) and F_2 = 153.864 kN (right) for four materials: (a) CA6NM, (b) A390 Al, (c) SS 314, (d) Structural Steel

The Von Mises equivalent stress distributions presented in Figure 3 illustrate the stress state for all four materials under the same loading conditions. Each of the stress maps exhibit a similar trend — that is, the peak stress for each of the four materials occurs at the location where the splitter root meets the bucket arm, which is a geometry-induced notch that will be a stress-raiser due to the impact loading of the jet stream. Additionally, from the location of maximum stress at the junction between the splitter root and the bucket arm, the Von Mises stress decreases in a monotonically decreasing manner towards the bucket lip. Finally, at each of the two load levels for the four materials, the peak Von Mises stress does not exceed the respective yield strength of each material, therefore confirming that the bucket is able to operate within the elastic limits of all four materials and that no permanent deformation will occur under the applied loads.

The most extreme loading condition applied to the bucket (horizontal bucket under combined static pressure and high force F_2) resulted in a maximum Von Mises stress of 88,000 Pa and maximum deformation was 25 mm. Even at this extreme limiting condition, the Von Mises stress is still over 3 orders of magnitude smaller than the yield strength of the weakest candidate material, A390 aluminium (yield strength = 180 MPa), establishing an exceptionally large structural safety factor for all four materials. Based on the results of this testing, it can be concluded that all four candidate materials are structurally adequate for the intended use.

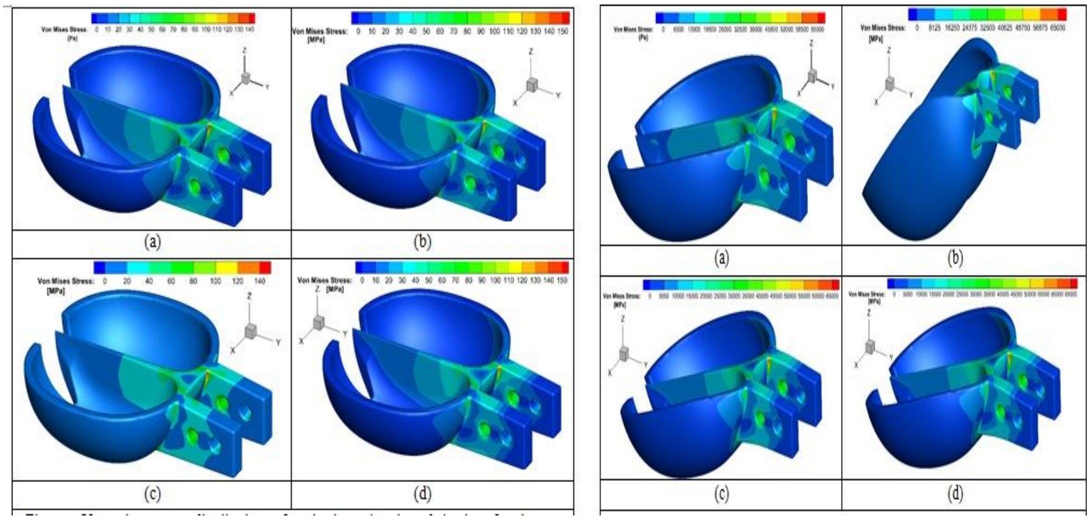

Figure 3 Von Mises equivalent stress distributions for horizontal bucket under F_1 = 349 N (left) and F_2 = 153.864 kN (right). Peak stress concentrations at the splitter-root junction remain below the yield strength of all four materials

Once Alan had performed a pre-stress modal analysis of the bucket, he was able to use the Block Lanczos extraction method to determine the natural frequencies of the bucket, and consequently, whether or not resonance conditions would exist when the bucket was operating under normal conditions. To calculate the bucket-passing frequency (the rate the buckets will intercept the water jet), use the following formula: $fb = Z \times N / 60 = 19 \times 1000 / 60 = 316.67$ Hz. The lowest natural frequency found for any of the buckets is 4,231.8 Hz, generating a resonance safety factor of 13.37. Additionally, each of the six buckets' modal frequencies will be much greater than any of the excitation frequencies and will be sufficiently spaced apart; therefore, there are no internal resonance concerns. The design is confirmed to be acoustically free of resonance for the entire operational speed range.

Based upon all the structural analyses performed, decided to use Stainless Steel 314 as the best material for the new bucket. The extreme corrosion resistance due to his high chromium content (i.e., 24-26%) makes it ideal for long-term water-side service; its yield strength of 586 MPa also provides ample safety against static overload; finally, the combination of the hardness and toughness of SS314 afford adequate resistance to fatigue and wear from over time due to exposure to muddy waters.

8.3 CFD Analysis

Steady-state computational fluid dynamics calculations were performed in ANSYS Fluent using a standard k-epsilon turbulence model with standard wall functions, with a tetrahedral mesh size of 0.5 mm having 403,167 nodes, and 2,183,335 elements. Inlet jet speeds of 15, 20, 35, 45, and 58.7 m/s were evaluated through the bucket (with zero gauge pressure outlet) under conditions of no-slip walls by means of computational simulations.

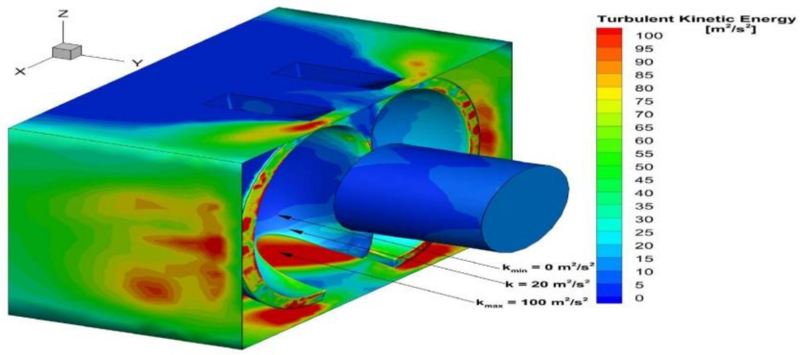

Figure 4 Turbulent kinetic energy (TKE) distribution within the Pelton bucket domain from steady-state CFD (k_max = 100 m^2/s^2). Highest TKE values at the splitter edge and jet-bucket interface indicate the zone of maximum kinetic-to-pressure energy conversion

Figure 4 shows the distribution of turbulent kinetic energy (TKE) in the bucket domain. The majority of the TKE is located at the splitter edge and at the junction of the jet and bucket, which is consistent with the basic understanding of the aerodynamics of impulse turbines; this is the area where the organized kinetic energy from the incoming jet quickly turns into turbulent fluctuations, which then turn into static pressure that drives the bucket. Although static pressure maps are not shown for brevity, they confirm that maximum static pressure exists at the splitter stagnation point and that there is a continuous decay of static pressure along the bucket contour from the inlet to the exit, which indicates effective and uniform transfer of momentum from the jet to the bucket.

CFD was performed with a transient analysis of an inlet velocity of 28 m/s, runner speed of 14.08 rad/s total mesh of 4,208,222 nodes and 21,670,542 elements with an interface for sliding mesh comparing symmetric jet bifurcation with a smooth flow attachment along an elliptical contour and no detectable flow separation..

8.4 Fabrication and Experimental Work

The enhanced Pelton turbine runner consisting of 14 buckets was created using 3D printed patterns as a prototype using sand casting technique utilizing Stainless Steel 314 material. This method ensures dimensional accuracy in the complex, bi-ellipsoidal bucket cavity that may have been impossible with Conventional, hand-carved wood patterns (including). Once cast, each individual bucket was machined to remove any excess material and had its surface inspected for any defects prior to being machined on their communicating surfaces. The completed 14 Bucket Runner Assembly (runner assembly) was then dynamically balanced utilizing a specific balance machine before being installed.

Figure 5 Fabricated Stainless Steel 314 enhanced Pelton bucket — individual buckets (left), buckets fitted on runner disc (centre), and completed 14-bucket runner assembly (right)

Five valve openings were evaluated for performance (20, 40, 60, 80 and 100 %) in a hydraulic testing facility. On the test rig, there was a single centrifugal pump calibrated Bourdon gauge for measuring the gauge pressure of the fluid at the system's inlet, and an inclined manometer for measuring the fluid velocity through the pitot tube, adjustable spear valve, (calibrated) spring balance and rope brake dynamometer to determine output power, digital tachometer for determining the speed of the pump's rotor.

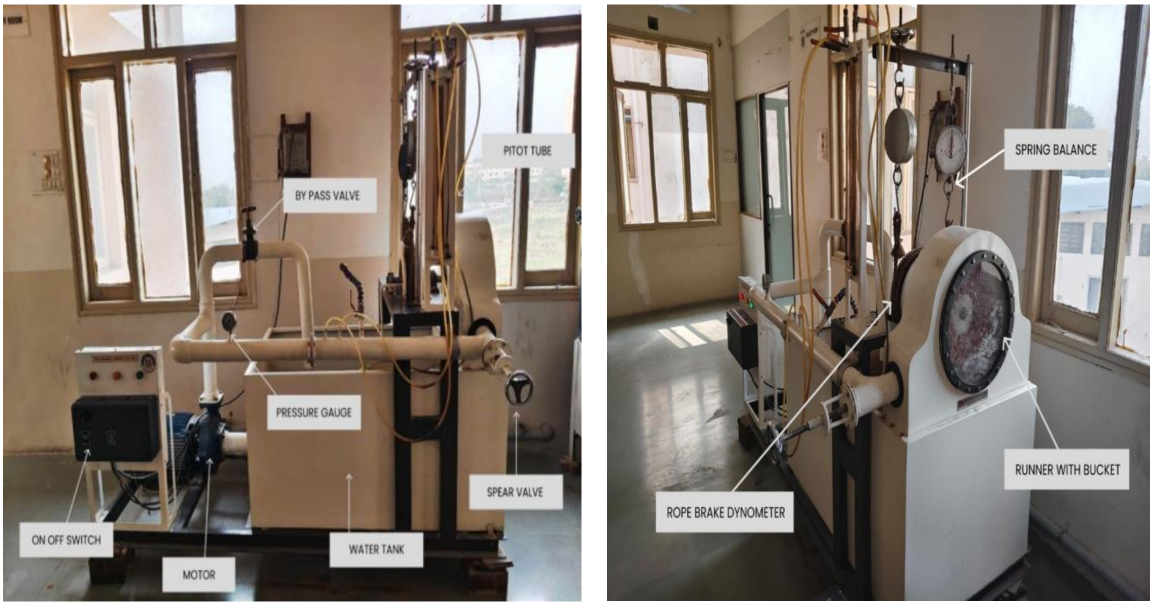

Figure 6 Experimental test Front view (left) — side view (left) front view (right)

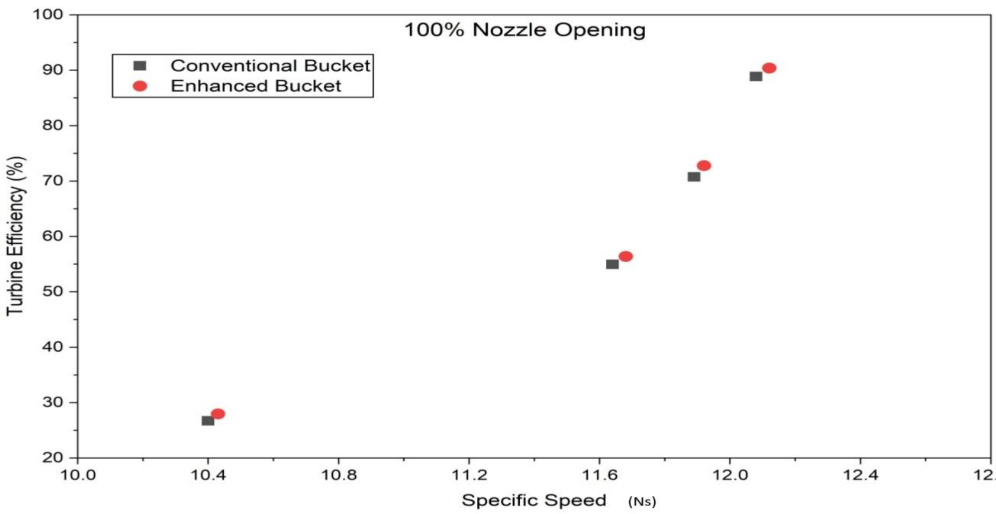

Figure 7 Specific speed versus Turbine efficiency at 100 percent nozzle opening for enhanced and conventional Pelton runners.

Figure 7 illustrates how efficient a specific speed is based on a nozzles fully open position. The Conventional and Enhanced of runners show an increase in efficiency with increasing specific speeds, which is as anticipated from turbine functionality. A maximum efficiency value of 90.92% occurs with enhanced runners (i.e., 2.05% greater than conventional) even when both types of runners are run in the same conditions. Additionally, the upward shift of the entire efficiency versus speed curve for enhanced runners throughout all of the specific speeds supports a trend to improve hydraulics across both narrow and wide efficiencies.

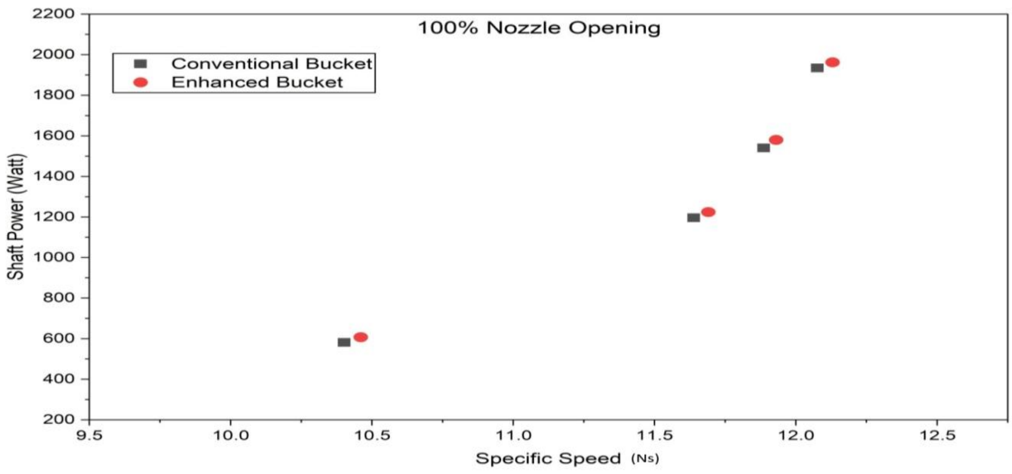

Figure 8 Specific speed versus shaft power at 100 percent nozzle opening.

Shaft power curves are depicted in Figure 8 The improved runner generates 2018.97 W of shaft power, 1,934.40 W generated by the Conventional runner. This is a net gain of 84.52 W, which equates to an improvement of 4.37%. In addition, at higher nozzle openings and higher specific speeds, the power advantage of the Enhanced runner is increased; therefore, the geometrical improvements made to the Enhanced runner will be most beneficial in the operating environment of maximum load for the turbine.

Table 4 Performance Comparison Enhanced Vs Conventional Runner at All Nozzle Openings

Nozzle	**Conventional η (%)**	**Enhanced η (%)**	**Δη (%)**	**Conventional P (W)**	**Enhanced P (W)**	**ΔP (%)**
20%	84.65	85.62	+0.97	1,667.12	1,682.30	+0.91
40%	86.28	87.46	+1.18	1,744.03	1,776.81	+1.88
60%	86.69	88.42	+1.73	1,689.70	1,737.49	+2.82
80%	86.70	88.67	+1.97	1,842.01	1,913.36	+3.87
100%	88.88	90.92	+2.05	1,934.40	2,018.97	+4.37

8. 5 Uncertainty Analysis

In accordance with ASME PTC 22-2014 and ISO GUM (JCGM 100:2008) [28], an of the combined performance results of the conventional and enhanced runner systems was performed to establish that the measured differences were not merely an artefact of experimental scatter, but had physical significance. Each derived quantity's combined standard uncertainty was calculated by propagating the aforementioned elemental measurement uncertainties (i.e., calibrated spring scale, Bourdon pressure gauge, digital tachometer, pitot tube flow measurement, and brake arm steel rule) through the efficiency and shaft power computational equations via the law of propagation of uncertainty.

At 100 percent nozzle opening, the combined uncertainty of hydraulic efficiency is ±1.83 percent (with a coverage factor $k = 2$ for 95 percent confidence). Since the measured efficiency improvement for the conventional runner and the enhanced runner system at 100 percent nozzle opening (2.05 percent) exceeds the combined uncertainty band, the enhancement is statistically significant. Conversely, the observed efficiency improvements at 20 percent and 40 percent nozzle openings (both < 1.20 percent), are both within the bounds of the combined uncertainty and therefore cannot be considered statistically significant. However, for 60 percent, 80 percent, and 100 percent nozzle openings, all of the efficiency improvements exceed the combined uncertainty bands, indicating real, repeatable hydraulic gains.

9. Conclusions

A. Design Optimization

• A systematic parametric study was conducted using the speed ratio and the bucket exit angle to establish optimal configurations for (φ = 0.485 and β=10 degrees), achieving maximum theoretical hydraulic efficiency of 94.29 percent.

• The design of the new bucket includes a 38.2 percent wider outer profile, resulting in improved jet capture and momentum transfer to the online comparison.

B. Structural FEA

• Static FEA determined that all four Different materials would possess full structural safety at all six loading conditions with the maximum Von Mises stress for any material being three magnitudes lower than its yield strength.

• Modal analysis prior to pre-loading confirmed that all four Different materials will be resonance-free with the minimum natural frequency being a factor of 13.4 greater than the bucket passing frequency. The optimal bucket material is Stainless Steel 314.

C. CFD Analysis

• CFD Analysis for steady state confirmed stagnation pressure at the splitter, smooth pressure decay along the bucket contour and maximum turbulent kinetic energy at the jet impingement zone; these findings are consistent with predicted velocity triangle results.

• CFD Analysis for transient with sliding mesh confirmed symmetric jet bifurcation, smooth attachment and no detectable separation, successfully validating the numerical model against experimental measurement data available from the literature.

D: Fabrication of Runner and Experimentation •

The enhanced runner was fabricated from Stainless Steel 314 using sand casting with 3D-printed patterns and was dynamically balanced before testing.

• Enhanced runner maximum hydraulic efficiency (90.92%) and maximum shaft power (2,018.97 W) were both higher than that of the conventional design by 2.05% (±2.05%) and 4.37% (±4.37%), respectively, at 100% nozzle opening.

APPENDIX A

PUBLICATION DETAILS

1. Chaudhari A. and Chaudhari G.C. (2023). “*Review on Micro Hydro Power Plant*”. In: Recent Advances in Fluid Dynamics, Lecture Notes in Mechanical Engineering. **Springer Nature** Singapore. Pages 401 to 409. DOI: 10.1007/978-981-19-3379-0_34.

2. Chaudhari A.H., Chaudhari G.C., and Bharti O.S. (2025). *“Performance of Pelton Turbine using ANSYS Mechanical APDL: Modal Analysis”*. Proceedings of the Institution of Mechanical Engineers **Part E: Journal of Process Mechanical Engineering. SAGE Publications.** DOI: 10.1177/09544089251334186.

3. Chaudhari A.H., Chaudhari G.C., and Bharti O.S. (2025) *“ Design Optimization of Micro-Hydro Pelton Turbine: Integration of Static and Modal Analysis Using ANSYS APDL. ”* **IOP Conference Series: Earth and Environmental Science.** Volume 1533, Article 012001. DOI: 10.1088/1755-1315/1533/1/012001.

4. Chaudhari A.H. and Chaudhari G.C. (2026). *“Optimization of Bucket Outlet Angle and Speed Ratio to Enhance the Efficiency of a Micro-Hydropower Plant. ”* **International Journal of Mechanical Engineering and Technology (IJMET)**. Volume 17, Issue 1, Pages 71 to 78. DOI: 10.34218/IJMET_17_01_005.

APPENDIX B

LIST OF REFERENCES

1. IEA (2021). Net Zero by 2050: A Road Map for the Global Energy Sector. International Energy Agency, Paris.

2. REN21 (2022). Renewables 2022 Global Status Report. Renewable Energy Policy Network for the 21st Century, Paris.

3. Ministry of New and Renewable Energy, Government of India (2025). Annual Report 2024-25. MNRE, New Delhi.

4. Central Electricity Authority, Government of India (2023). Optimal Generation Mix Report 2029-30. CEA, New Delhi.

5. AHEC, IIT Roorkee (2016). Small Hydro Database of India — July 2016 Edition. Alternate Hydro Energy Centre, Roorkee.

6. Ministry of Power, Government of India (2023). Guidelines to Promote Development of Pumped Storage Projects (PSP).

7. Lester A. Pelton (1880). Water Wheel. US Patent 233692.

8. Wagner H.-J. and Mathur J. (2011). Introduction to Hydro Energy Systems. Springer Berlin Heidelberg. DOI: 10.1007/978-3-642-20709-9.

9. Han F.Q. et al. (2011). Unsteady separation of jet branch by cutout of rotating Pelton bucket. Science China Technical Sciences, 54, pp. 302-310.

10. Alnakhlani M.M. et al. (2015). Effect of Bucket and Nozzle Dimension on Performance of a Pelton Water Turbine. Modern Applied Science, 9(1). DOI: 10.5539/mas.v9n1p25.

11. Kim J.-W. et al. (2017). Theoretical method of selecting number of buckets for a Pelton turbine. Journal of Hydraulic Research, 55(5), pp. 695-705.

12. Rossetti A. et al. (2013). Influence of bucket geometry on Pelton performance. Proceedings of the IMechE Part A, 228, pp. 33-45.

13. Sharma V. and Dhama S.K. (2014). Analysis of Stress on Pelton Turbine Blade Due to Jet Impingement. Int. J. Current Engineering and Technology, 4(4), pp. 2414-2417.

14. Rai A.K. et al. (2016). Forces acting on particles in a Pelton bucket and similarity considerations for erosion. IOP Conf. Series: Earth and Environmental Science, 49, 122002.

15. Padhy M.K. and Saini R.P. (2012). Study of silt erosion mechanism in Pelton turbine buckets. Energy, 39, pp. 286-293.

16. Patel K. et al. (2010). Development of Pelton turbine using numerical simulation. IOP Conf. Series: Earth and Environmental Science, 12, 012048.

17. Zidonis A. and Aggidis G.A. (2016). Pelton Turbine: Identifying the Optimum Number of Buckets using CFD. Journal of Hydrodynamics, 28(1), pp. 75-83.

18. Nigussie T. et al. (2017). Design, Modeling, and CFD Analysis of a Micro Hydro Pelton Turbine Runner. International Journal of Rotating Machinery, 2017, Art. 3030217.

19. Zidonis A. and Aggidis G.A. (2015). State of the art in numerical modelling of Pelton turbines. Renewable and Sustainable Energy Reviews, 45, pp. 135-144.

20. Petley S. and Aggidis G.A. (2019). Transient CFD and experimental analysis for improved Pelton turbine casing designs. IOP Conf. Series: Earth and Environmental Science, 240, 022005.

21. Gupta V. et al. (2016). Numerical simulation of six jet Pelton turbine model. Energy, 104, pp. 24-32.

22. Chaudhari G.C. (2016). Numerical, Experimental and Flow Visualization Studies on Conventional and Hooped Pelton Turbine Runner. PhD Thesis, SVNIT, Surat.

23. Shah H.A., Chaudhari G.C., and Dhiman V.D. (2021). Parametric Optimization and Design of Pelton Turbine Wheel for Hydraulic Efficiency Improvement. Journal of Physics: Conference Series, 2007(1), 012019.

24. Chaudhari A.H., Chaudhari G.C., and Bharti O.S. (2025). Performance of Pelton Turbine using ANSYS Mechanical APDL: Modal Analysis. Proceedings of the IMechE Part E. DOI: 10.1177/09544089251334186.

25. Perrig A. (2007). Hydrodynamics of the free surface flow in Pelton turbine buckets. PhD Thesis, EPFL, Lausanne. DOI: 10.5075/epfl-thesis-3715.

26. Cimbala J. and Cengel Y. (2019). Fluid Mechanics. McGraw Hill, India.

27. Bhattarai S. et al. (2019). Novel trends in modelling techniques of Pelton Turbine bucket. Renewable and Sustainable Energy Reviews, 112, pp. 87-101.

28. JCGM 100:2008 and ASME PTC 22-2014. Guide to the Expression of Uncertainty in Measurement (GUM). Joint Committee for Guides in Metrology, BIPM.

29. Spencer, T., Rodrigues, N., Pachouri, R., and Thakre, S. *A Model-Based Assessment of Variable Renewable Grid Integration Costs in India*. The Energy and Resources Institute, New Delhi, 2021.

30.Lester Allan Pelton. *Improvement in Water-Wheels and Turbines*. U.S. Patent No. 233692, 1880.

31. S. Anagnostopoulos. *Numerical Study of Flow in a Pelton Turbine Runner Using CFD*. Journal of Hydrodynamics, 2010.